HHS Public Access

Author manuscript

Neuroscience. Author manuscript; available in PMC 2024 January 01.

Published in final edited form as:

Neuroscience. 2023 January 01; 508: 98–109. doi:10.1016/j.neuroscience.2022.08.020.

Doublecortin-like kinase 1 (DCLK1) Facilitates Dendritic Spine Growth of Pyramidal Neurons in Mouse Prefrontal Cortex

Kelsey E. Murphy,

Erin Y. Zhang,

Elliott V. Wyatt,

Justin E. Sperringer,

Bryce W. Duncan,

Patricia F. Maness

Department of Biochemistry and Biophysics, and Carolina Institute of Developmental Disabilities, University of North Carolina School of Medicine at Chapel Hill

Abstract

The L1 cell adhesion molecule NrCAM (Neuron-glia related cell adhesion molecule) functions as a co-receptor for secreted class 3 Semaphorins to prune subpopulations of dendritic spines on apical dendrites of pyramidal neurons in the developing mouse neocortex. The developing spine cytoskeleton is enriched in actin filaments, but a small number of microtubules have been shown to enter the spine apparently trafficking vesicles to the membrane. Doublecortin-like kinase 1 (DCLK1) is a member of the Doublecortin (DCX) family of microtubule-binding proteins with serine/threonine kinase activity. To determine if DCLK1 plays a role in spine remodeling, we generated a tamoxifen-inducible mouse line (Nex1Cre-ERT2: DCLK1$^{flox/flox:}$ RCE) to delete microtubule binding isoforms of DCLK1 from pyramidal neurons during postnatal stages of spine development. Homozygous DCLK1 conditional mutant mice exhibited decreased spine density on apical dendrites of pyramidal neurons in the prefrontal cortex (layer 2/3). Mature mushroom spines were selectively decreased upon DCLK1 deletion but dendritic arborization was unaltered. Mutagenesis and binding studies revealed that DCLK1 bound NrCAM at the conserved FIGQY^{1231} motif in the NrCAM cytoplasmic domain, a known interaction site for the actin-spectrin adaptor Ankyrin. These findings demonstrate in a novel mouse model that DCLK1 facilitates spine growth and maturation on cortical pyramidal neurons in the mouse prefrontal cortex.

Graphical Abstract

Corresponding author: Patricia F. Maness, PhD, Professor, UNC Chapel Hill, **Address:** Department of Biochemistry and Biophysics, University of North Carolina School of Medicine at Chapel Hill, Campus Box 7260, Chapel Hill, NC 27599, 919-966-3532 office, 919-962-8326 fax, srclab@med.unc.edu.

Conflict of interest statement:
The authors declare no conflicts of interest in publication of this manuscript

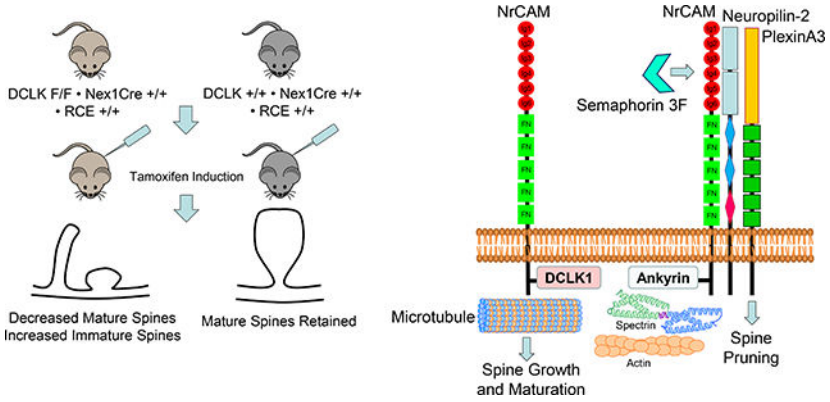

Keywords

Doublecortin-like kinase; dendritic spines; cortical pyramidal neurons; NrCAM; Ankyrin; mouse models

Introduction

Dendritic spine remodeling in developing pyramidal neurons is important for establishing an appropriate level of excitatory connections in the neocortex. The L1 family cell adhesion molecules Neuron-glia related protein (NrCAM) and Close Homolog of L1 (CHL1) mediate selective pruning of dendritic spine subpopulations in the mouse neocortex in response to class 3 secreted Semaphorins (Sema3s) through an activity dependent mechanism (Tran *et al.*, 2009;Mohan *et al.*, 2019a;Mohan *et al.*, 2019b). Heterotrimeric receptors comprising L1-CAMs, Neuropilins (Npn1–2), and PlexinAs (PlexA1–4) transduce Sema3 signals to achieve selective spine pruning (Duncan *et al.*, 2021a;Duncan *et al.*, 2021b). All L1-CAMs share a conserved cytoplasmic domain containing the motif FIGQY (FIGAY in CHL1) that binds the actin-spectrin adaptor protein Ankyrin when the tyrosine (Y) residue is not phosphorylated (Bennett and Healy, 2009).

Doublecortin-Like Kinase 1 (DCLK), a member of the doublecortin (DCX) family, is a microtubule-associated protein with serine/threonine kinase activity, important for microtubule bundling and linkage to F-actin (Friocourt *et al.*, 2007;Yap *et al.*, 2012;Yap and Winckler, 2015;Lipka *et al.*, 2016). DCLK1 on human chromosome 13 is associated with schizophrenia (Havik *et al.*, 2012), whereas X chromosome mutations in DCX result in lissencephaly (smooth brain) and a double-layered cortex, producing intellectual disability (des Portes *et al.*, 1998). Recently, DCLK1 was reported to regulate the levels of α-Synuclein, a protein that induces neurotoxicity at increased levels, and may drive a genetic form of Parkinson's Disease (Vazquez-Velez *et al.*, 2020). DCX contains two microtubule binding domains and a serine/proline rich PEST (proline, glutamate, serine, threonine) sequence (Fig. 1A). DCLK1 (82 kDa) also has two microtubule binding domains and the PEST sequence, as well as a carboxyl terminal serine/threonine protein kinase domain. Alternative splicing of the DCLK1 gene generates a DCX-like isoform of 40 kDa, lacking the kinase domain, while alternative promoter usage generates a short isoform, DCLK1-S (42 kDa), lacking the microtubule binding domains. Substrates of

DCLK1 are poorly defined but include DCLK1 itself, which inhibits microtubule bundling and polymerization (Patel *et al.*, 2016), and microtubule associated protein 7 domain 1 (MAP7D1), which promotes axon elongation (Koizumi *et al.*, 2017). Several lines of evidence suggest that DCLK1 may regulate spine morphogenesis. (a) DCLK1 is present in the somatodendritic region of neurons (Shin *et al.*, 2013) and transports KIF1-mediated cargo of dense core vesicles along microtubules to increase dendrite growth (Lipka *et al.*, 2016). (b) Microtubules have been shown to invade spines for protein and vesicle transport via kinesin to facilitate synaptic plasticity (McVicker *et al.*, 2016;Dent, 2017). (c) DCLK1 knockdown by shRNA in embryonic neural progenitors decreases dendritic arborization and alters spine morphology (Shin *et al.*, 2013). Although global knockout of DCLK1 in mice showed intact neuronal migration, cortical thickness, and lamination, subtle phenotypic changes in neurons, including spine density, were not examined (Deuel *et al.*, 2006;Shin *et al.*, 2013).

To investigate a function for DCLK1 in postnatal cortical pyramidal neurons, we generated an inducible, conditional mouse line (Nex1Cre-ERT2: DCLK1$^{flox/flox:}$ RCE) targeting the principal microtubule binding isoforms. Tamoxifen induction of the CreERT2 recombinase under control of the Nex1 promoter achieves cell-specific targeting of postmitotic cortical and hippocampal pyramidal neurons with no detectable targeting of interneurons, oligodendroglia, astrocytes, or non-neural cells (Agarwal *et al.*, 2012). By introducing tamoxifen at early postnatal stages gene excision can be restricted to post migratory pyramidal neurons, circumventing effects on migration and cortical positioning. This induction regimen was applied during the active period of spine remodeling (P10-P13) in Nex1Cre-ERT2: DCLK1$^{flox/flox:}$ RCE mice enabling examination of DCLK1 function in dendritic spine regulation in postmitotic pyramidal neurons.

Homozygous recombination of DCLK1 in Nex1Cre-ERT2: DCLK1$^{flox/flox}$: RCE mice during postnatal spine remodeling decreased DCLK1 expression, spine density and mature morphology on apical dendrites of pyramidal neurons in the mouse prefrontal cortex. In addition, DCLK1 bound the neural adhesion molecule NrCAM, a known regulator of spine density (Demyanenko *et al.*, 2014;Mohan *et al.*, 2019a), and specifically targeted the Ankyrin interaction motif (FIGQY) in the NrCAM cytoplasmic domain. Generation of an inducible mouse model for DCLK1 in pyramidal neurons, and identification of a novel role for DCLK1 in dendritic spine regulation contributes to our understanding of postnatal brain development and may shed light on pathological mechanisms associated with its dysfunction.

Experimental Procedures

Generation and tamoxifen induction of DCLK1 conditional mutant mice

A conditional, inducible DCLK1 mouse line (Nex1Cre-ERT2: DCLK1$^{flox/flox:}$ RCE) was generated, in which DCLK1 can be deleted in pyramidal neurons of the neocortex and hippocampus under control of the Nex1Cre-ERT2 promoter by tamoxifen treatment at specific times in development. The Nex1 promoter drives the tamoxifen-inducible Cre-ERT2 recombinase only in post-mitotic pyramidal neurons (Goebbels *et al.*, 2006;Agarwal *et al.*,

2012). Other investigators have also used Nex1-Cre mice to specifically target postmitotic pyramidal neurons (Golonzhka *et al.*, 2015;Fame *et al.*, 2016;Miller and Wright, 2021).

As shown in Fig. 1B, Nex1Cre-ERT2 mice (from Amit Agarwal) were first intercrossed with RCE: loxP mice (from Gordon Fishell) so that expression of Cre causes recombination of a “floxed stop cassette” allowing EGFP expression (Sousa *et al.*, 2009). Nex1Cre-ERT2: RCE mice were then intercrossed with DCLK1$^{tm1.2jgg}$ mice containing floxed exon 3, the second coding exon of DCLK1, on a mixed genetic background of C57/Bl6, 129 and Black Swiss (Jackson Laboratory strain 013170; (Koizumi *et al.*, 2006)), Joseph Gleeson, donating investigator). Cre-mediated recombination has been shown to delete exon 3, eliminating expression of full length DCLK1 (82K) and the alternatively spliced DCX-like variant (40 kDa) lacking the kinase domain (Koizumi *et al.*, 2006). Subsequent breeding produced Nex1Cre-ERT2: RCE mice with DCLK1$^{flox/flox}$, DCLK1$^{flox/+}$, and DCLK1$^{+/+}$(wild type, WT) genotypes in expected ratios. Each allele was genotyped by PCR from tail DNA (Fig. 1D). For *in vivo* induction, tamoxifen (Sigma-Aldrich, #10540–29-1) was dissolved (10 mg/ml) in sunflower seed oil (Sigma, S5007), and administered by intraperitoneal injection at 100 mg/kg body weight every 24 hours for 4 consecutive days. Balanced sexes of male and female mice were used in the present studies. Mice were maintained according to policies of the University of North Carolina Institutional Animal Care and Use Committee (IACUC; AAALAC Institutional Number: #329; ID# 18–073, 21–039) in accordance with NIH guidelines. Genotyping was performed by PCR.

Immunoreagents

Rabbit polyclonal antibodies against the carboxyl-terminal region (residues 700 to C-terminus) of mouse DCLK1 (Abcam, # ab31704) recognize full length DCLK1 and the short isoform DCLK1-S. These antibodies have been knockout validated. Polyclonal antibodies against NrCAM (Abcam #24344) or R&D Systems (Abcam #8538) and GFP (Abcam #13970) were also used. Non-immune rabbit IgG (NIg), HRP- and Alexa Fluor (488 and 555) conjugated secondary antibodies were from Jackson Immunoresearch.

Analysis of DCLK1 immunolabeling, spine density, morphology, and dendritic branching

Mice (P19-P34) were anesthetized with 2.5% Avertin, perfused transcardially with 4% paraformaldehyde (PFA)/PBS and processed for staining as described (Demyanenko *et al.*, 1999). Brains were postfixed in 4% PFA overnight at 4°C, followed by 0.02% PBS-azide, then sectioned coronally on a vibratome (60 μm) and mounted on glass slides. Sections were permeabilized in 0.3% Triton X-100 and blocked in 10% normal donkey serum in PBS for 3 hours at room temperature. Sections were incubated with chicken anti-GFP (1:250) and anti-DCLK1 antibodies (1:250) for 48 hours at 4°C. After washing, sections were incubated with anti-chicken Alexa Fluor-488 or anti-rabbit Alexa Fluor-555 secondary antibodies (1:250) for 2 hours before mounting with Prolong Glass (Thermofisher). Confocal z-stacks were obtained by imaging on a Zeiss LSM 700 microscope in the UNC Microscopy Services Laboratory with an EC Plan Neofluar 40x objective with a 1.3 N.A. oil lens. Images were acquired using a pinhole size of 1 AU. Zoom was adjusted to obtain pixel sizes of 0.13–0.14 μm. DCLK1 pixel intensities were quantified within the neuropil and soma combined from TIF images of confocal maximum intensity projections in FIJI. Regions of interest (ROIs)

were selected using a grid, and mean grey values obtained using the Analysis menu in FIJI to yield pixel intensities. Pixel intensities of negative control staining with secondary antibodies alone were obtained similarly to determine the background fluorescence, which was subtracted from mean pixel intensities of DCLK1 immunofluorescence. The resulting mean pixel intensity per unit area for each genotype was plotted as a histogram, and compared by the t-test for significant differences ($p < 0.05$).

Spine density of layer 2/3 pyramidal neurons in the prefrontal cortex (primary cingulate area) was quantified using Neurolucida software (MBF Bioscience) as described (Demyanenko *et al.*, 2014;Mohan *et al.*, 2019a;Mohan *et al.*, 2019b). Briefly, spines were traced and quantified blind to observer on 30 μm segments of the first branch of apical or basal dendrites from confocal z-stack images after deconvolution. For image deconvolution and 3D reconstructions, dendritic z-stacks were deconvolved using Auto Quant 3 software (Media Cybernetics) with default deconvolution settings in Imaris (Bitplane). Mean spine number per 10 μm of dendritic length (density) was calculated. Approximately 39–49 neurons/mouse were analyzed (39 DCLK1 +/+ neurons, 44 DCLK1 F/+ neurons, and 49 DCLK1 F/F neurons) from 4–6 mice/genotype; P19-P34). Mean spine densities/10 μM ± SEM were compared across genotypes by two-factor ANOVA and Tukey's posthoc testing for multiple comparisons, with significance set at $p<0.05$.

Spine morphologies were scored on 3D reconstructed images as mature (mushroom) or immature (stubby and thin/filopodial) on apical dendrites as defined (Peters and Kaiserman-Abramof, 1970;Peters and Harriman, 1990) and reported previously (Mohan *et al.*, 2019a). To compare spine morphologies of DCLK1 +/+ and DCLK1 F/F mice, spine morphological types were scored on the primary branch of apical dendrites in 17–19 neurons/genotype, and the fraction of mature or immature spines was calculated relative to total spines. The mean fraction of mature (mushroom) spines and immature (thin and stubby) spines per genotype was plotted on a histogram, and compared for statistical significance by the Mann-Whitney t-test (2-tailed, unequal variance, $p < 0.05$).

Dendritic arborization was measured by Sholl analysis in pyramidal neurons of the cingulate cortex in DCLK1 +/+ and DCLK1 F/F mice (P19-P34, n= 3 mice/genotype) induced at P10-P13. The number of processes crossing concentric rings centered on the soma of EGFP-labeled pyramidal neurons (approximately 15 neurons/genotype) was scored in confocal z-stacks (20x). The center was defined as the middle of the cell body at a soma detector sensitivity of 1.5 μm, and the automatic tracing mode of Neurolucida was used to seed and trace dendritic arbors. Images in DAT format were subjected to Sholl analysis using Neurolucida Explorer with a starting radius of 10 μm and radial increments of 10 μm ending at 130 μm. Sholl data were compared between genotypes using paired t-tests for differences in the mean number of dendrite intersections at each distance from the soma ($p< 0.05$).

For estimating the size of major axonal tracts (corpus callosum and anterior commissure) in DCLK1 +/+, F/+, and F/F mice (3–5 mice/genotype; P19-P34), serial coronal brain sections were made, imaged on the confocal microscope (5x), and analyzed in FIJI. The dorsoventral width of each tract was measured at the midline of each section, and the mean width

calculated. Means were compared by 1 factor ANOVA with Tukey's posthoc comparisons ($p < 0.05$).

Immunoprecipitation and immunoblotting

Protein-protein interactions were assessed by co-immunoprecipitation and immunoblotted from transfected HEK293T cells, mouse forebrain, and synaptoneurosomes. HEK293T cells were grown in DMEM, gentamicin, kanamycin,10% FBS in a humidified incubator with 5% CO_2. Cells were seeded at 2×10^6 cells/100mm dish the day before transfection. Plasmids expressing WT or mutant NrCAM cDNA were cotransfected with either Ankyrin B or DCLK1 at a 2:1 molar ratio with Lipofectamine 2000 (ThermoFisher, #11668) in Opti-MEM. Media was changed to complete DMEM after 18 h, and cells were lysed and collected 48 h post-transfection. Cells were harvested in 20 mM Tris, pH 7.0, 150 mM NaCl, 200 μM Na_3VO_4, 1 mM NaEGTA, 1% Triton X-100, 10 mM NaF, 1x protease inhibitor cocktail (Sigma Aldrich #P8340). For preparation of mouse cortical lysates, mouse forebrains were dissociated and subjected to Dounce homogenization for 20 strokes in RIPA buffer. Homogenates were incubated for 15 minutes on ice, then centrifuged at 16,000 × g for 10 minutes. Supernatants were retained and protein concentrations determined by BCA.

Synaptoneurosomes were isolated as described (Villasana *et al.*, 2006) with modifications (Demyanenko *et al.*, 2014). WT mice (P32) were anesthetized, decapitated and cortices isolated. Briefly, cortices were subjected to Dounce homogenization in 10 mM HEPES, pH 7.0, 1 mM NaEDTA, 2 mM NaEGTA, 2 mM NaF, 1x protease inhibitor cocktail, sonicated, and filtered through a 100 μm cell strainer followed by a 5 μm filter in a media filtration device (VWR, #1101). The filtered homogenate was centrifuged at 1000 × g for 10 min to produce supernatant S1. The S1 fraction was centrifuged at 10,000 × g for 15 min to produce a pellet that represented the crude synaptosome fraction. This fraction was washed once, lysed in 20 mM Tris-HCl, pH 7.4, 150 mM NaCL, 5 mM NaEDTA, 2 mM NaEGTA, 1% (v/v) Triton X-100, 2 mM NaF, 1X protease inhibitor cocktail, followed by centrifugation at 16,000 × g for 10 minutes at 4°C. The supernatant was retained as the synaptoneurosome fraction. Synapse-associated protein 102 (SAP102) and postsynaptic density protein 95 (PSD95) were enriched in the synaptoneurosome fraction over the S1 fraction as shown by Western blotting.

For immunoprecipitation, lysates of mouse forebrain (1 mg) or HEK293T cells (0.5 mg) were precleared for 30 minutes at 4°C using Protein A/G Sepharose beads (ThermoFisher). Precleared lysates (equal amounts of protein) were incubated with 3 μg rabbit polyclonal antibody to NrCAM (Abcam #24344) or NIg for 2 h r on ice. Protein A/G Sepharose beads were added for an additional 30 min with nutation at 4°C before washing with RIPA buffer or Triton lysis buffer (synaptoneurosomes). Beads were washed 4 times, then immunoprecipitated proteins were eluted from the beads by boiling in SDS-PAGE sample buffer. Samples (50 μg) were subjected to SDS-PAGE (6%) and transferred to nitrocellulose. Membranes were blocked in TBST containing 5% nonfat dried milk and incubated overnight with primary antibodies (1:1000), washed, and incubated with HRP-secondary antibodies (1:5000) for 1 h. Antibodies were diluted in 5% milk/Tris buffered saline/0.1% Tween-20 (TBST). Blots were developed using Western Bright ECL Substrate (Advansta) and exposed

to film for times yielding a linear response of signal. Membranes were stripped and reprobed with rabbit anti-NrCAM antibodies (R&D Systems AF8538) or antibodies to loading control proteins actin or vinculin. Bands on Western blots were measured from TIF images obtained by densitometric scanning in FIJI on regions of interest (ROIs) framed using the rectangle tool. Background densities were obtained with the same frames above or below the protein band, and subtracted. Ratios of the protein bands and loading controls were calculated and means ± SEM obtained from replicate experiments.

Results

Characterization of Nex1Cre-DCLK1 mutant mice

To identify functional effects of postnatal DCLK1 deletion on dendritic spine development in cortical pyramidal neurons, we generated a tamoxifen-inducible mouse line, Nex1Cre-ERT2: DCLK1$^{flox/flox:}$ RCE (Fig.1B). In these mice, floxed exon 3 in the DCLK1 gene was excised by tamoxifen-induced loxP recombination under control of the Nex1 promoter (Agarwal *et al.*, 2012;Mohan *et al.*, 2019a). Nex1 encodes a neuronal basic helix-loop-helix protein whose expression is restricted to postmitotic pyramidal neurons in the neocortex and hippocampus. Nex1Cre-ERT2 mice represent an established line expressing Cre recombinase fused to the ligand-binding domain of the estrogen receptor under control of the endogenous Nex1 promoter (Goebbels *et al.*, 2006;Agarwal *et al.*, 2012). The Cre-ERT2 gene was knocked into the Nex1 locus enabling inducible Cre expression in postnatal pyramidal neurons and deletion of floxed alleles in response to tamoxifen. Induction of Nex1Cre-ERT2 recombination was shown to be restricted to postmitotic pyramidal neurons and does not occur in neural progenitors, interneurons, oligodendroglia, or astrocytes (Agarwal *et al.*, 2012). In the present study neurons undergoing recombination for DCLK1 express EGFP from the RCE: loxP cassette (Sousa *et al.*, 2009), which is also induced by Cre-ERT2 in response to tamoxifen.

Exon 3 excision in EIIa-Cre: DCLK1 F/F mice has been shown to eliminate the DCLK1 isoforms with microtubule binding domains: full length DCLK1 (82 kDa) and DCX-like splice variant (40 kDa) (Koizumi *et al.*, 2006). The kinase-only short isoform (DCLK1-S; 42 kDa) generated from alternative promoter usage is not deleted (Koizumi *et al.*, 2006). DCLK1-S, also called CPG16 (Nedivi *et al.*, 1993), is expressed exclusively in adult brain and at much lower levels than the full length isoform. In our studies mice were injected with tamoxifen in the juvenile period (P10-P13), when cortical layers 2–4 have mostly formed, in order to delete the microtubule binding isoforms of DCLK1 during the most active stages of spine formation and remodeling (Culotta and Penzes, 2020). To achieve recombination, mice were given daily tamoxifen injections intraperitoneally from P10 to P13 as described (Agarwal *et al.*, 2012;Mohan *et al.*, 2019a), resulting in permanent loss of the targeted DCLK1 isoforms. Use of the Nex1Cre-ERT2 promoter avoided deleting DCLK1 in immature progenitors, unlike Nestin or EIIa promoters. Our analysis focused on pyramidal neurons in the prefrontal cortex, because of their importance in social and cognitive circuits that may be altered in DCLK1-linked neurological disease (Yizhar, 2012;Kroon *et al.*, 2019).

Tamoxifen induction at P10-P13 resulted in expression of EGFP, indicating recombination, in pyramidal neurons throughout layers 2–6 in the primary cingulate area (Cg1) of the medial prefrontal cortex of Nex1Cre-ERT2: DCLK+/+: RCE ("WT", termed DCLK1 +/+), heterozygous Nex1Cre-ERT2: DCLK1$^{flox/+}$: RCE (termed F/+), and homozygous Nex1Cre-ERT2: DCLK1$^{flox/flox}$: RCE mice (termed F/F) (Fig. 1C). Mice were genotyped by PCR (Fig.1D). We focused our analysis on mice at P19-P34, a juvenile to adolescent stage as defined by (Laviola *et al.*, 2003). Prior to and overlapping with this time frame, overproduced dendritic spines are pruned to appropriate levels. Spine turnover decreases substantially from P19-P34 as mature circuits are stabilized (Trachtenberg *et al.*, 2002;Holtmaat A. J. *et al.*, 2005).

Expression of DCLK1 protein in layer 2/3 of Cg1 was decreased in DCLK1 F/F compared to DCLK1 +/+ mice, as evident from DCLK1 immunofluorescence (red) in EGFP-labeled cell bodies and neuropil (combined) in confocal images (Fig. 1 E.F). The level of DCLK1 immunofluorescence alone (single channel) was clearly higher in DCLK1 +/+ compared to DCLK1 F/F cortex (Fig. 1 G,H). The insert in Fig. 1G shows negative control immunostaining with secondary antibodies and demonstrates that the staining in both genotypes is clearly above background. Quantitation of single channel DCLK1 fluorescence pixel intensity in the DCLK1 F/F Cg1 (Fig. 1I) was significantly reduced (1899 ± 77 mean pixel intensity/unit area) compared to DCLK+/+ Cg1 (2497 ± 63, t-test, *p<0.0001) in multiple images from 3 mice/genotype. The decrease was approximately 24% lower in mutant than DCLK1 +/+. Antibodies used for immunostaining recognized the DCLK1 carboxyl terminus, which is shared by DCLK1 (82 kDa) and DCLK1-S (42K). Therefore some of the residual staining in the mutant brain may be due to DCLK-S, as well as to any non-recombined pyramidal neurons or other cell types. DCLK1 staining in the mutant Cg1 may also be derived from interneuron processes, glia, and axons of neurons from subcortical regions (amygdala, ventral tegmental area, etc.), the latter of which do not express Nex1 and therefore would not undergo DCLK1 deletion. DCLK1 in the mouse cortex is known to be expressed in excitatory and inhibitory neurons, as well as astrocytes and oligodendroglia (Allen Brain Map Transcriptomics Explorer: (https://celltypes.brain-map.org/rnaseq/mousectx-). Western blotting of DCLK1 in cortical lysates from DCLK1+/+ and DCLK1 F/F mice showed a mean decrease of approximately 23% in the DCLK182 kDa isoform in the mutant relative to the vinculin (124 kDa) loading control (Fig. 1J) in accord with the decrease in DCLK1 immunostaining. The DCLK1 42 kDa isoform was too light to be reliably quantified. DCLK1 antibodies were used for immunostaining of dissociated cortical neurons expressing EGFP from a transfected pCAG-IRES-EGFP plasmid in culture at DIV14. DCLK1 immunolabeling was evident on EGFP-labeled dendritic shafts and spines in confocal images, but was not enriched in spines compared to dendrites, as shown in Fig. 1 K.

Postnatal deletion of DCLK1 from cortical pyramidal neurons decreases spine density and alters spine morphology

To investigate an *in vivo* role for DCLK1 in regulating spine density in the prefrontal cortex, recombination was induced in DCLK1 +/+, F/+ and F/F mice at P10-P13, and spine density was analyzed on EGFP-positive apical dendrites of pyramidal neurons in layer 2/3 of Cg1

at P19-P34 (Fig. 2A). Apical dendrites were analyzed because spines on apical but not basal dendrites are selectively regulated by L1-CAMs (Duncan *et al.*, 2021b), which may interact with DCLK1. In immunostaining experiments of mouse brain it was reported that DCLK1 codistributes with L1, the prototype of the L1-CAM family, on axon tracts but is more widespread (Koizumi *et al.*, 2006). Spine density was significantly decreased on apical dendrites of cortical pyramidal neurons in DCLK1 F/F compared to DCLK1 +/+ mice (* 1-factor ANOVA with Tukey's posthoc comparisons) (Fig. 2B). DCLK1 F/+ mice also exhibited significantly decreased spine density compared to DCLK1 +/+ mice or to DCLK1 F/F mice (Fig. 2B). In summary, the findings suggested that DCLK1 is required to facilitate spinogenesis or maintenance in postnatal pyramidal neurons in the prefrontal cortex.

Dendritic spine morphology can be classified based on size and shape (mushroom, stubby, and thin), reflecting the degree of maturity, dynamics, and functional properties (Peters and Kaiserman-Abramof, 1970). Immature spines (stubby and thin) are associated juvenile plasticity and have been termed "learning spines" (Bourne and Harris, 2007), while mushroom spines ("memory spines") are associated with mature synapses (Bhatt *et al.*, 2009;Holtmaat A. and Svoboda, 2009;Berry and Nedivi, 2017). Deletion of DCLK1 at P10–13 significantly decreased the fraction of mature mushroom spines on apical dendrites of layer 2/3 pyramidal neurons in the prefrontal cortex of DCLK1 F/F mice compared to DCLK1 +/+ mice at P19-P34 (* Mann-Whitney, 2-tailed t-test) (Fig. 2 C). There was also a significant increase in the fraction of immature spines (thin and stubby) in DCLK1 F/F compared to DCLK1 +/+ mice (Fig. 2C).

Sholl analysis was carried out to evaluate any changes in branching of dendritic processes of layer 2/3 pyramidal neurons in the prefrontal cortex (P19-P34) following DCLK1 deletion and expression of EGFP at P10-P13. Representative low magnification images are shown in Fig. 1D. No significant differences were observed in branching of DCLK1 +/+ and DCLK1 F/F dendritic arbors at distances up to 130 μm from the soma (paired t-tests for mean number of dendrite crossings at each distance) (Fig. 2 E). Limitations of dendrite tracing in GFP-expressing neurons in cortical sections at greater distances precluded full analysis of terminal branching.

In homozygous DCLK1 F/F or heterozygous DCLK1 F/+ mice, tamoxifen induction at P10-P13 did not cause gross neuroanatomical defects or alterations in the size of large axonal tracts, in particular the corpus callosum and anterior commissure (Fig. 2 F,G). There was no significant differences in the width of the corpus callosum or anterior commissure at the midline among DCLK1 +/+, DCLK1 F/+, and DCLK1 F/F mice (1 factor ANOVA with Tukey's post hoc comparisons; $p > 0.05$). Cortical thickness and lamination, and size of the hippocampus and brain ventricles also appeared unaltered in the mutant mice, and other neuroanatomical abnormalities were not apparent, in agreement with the phenotype of DCLK1 global knockout mice (Deuel *et al.*, 2006).

DCLK1 expression and association with NrCAM at the FIGQY motif

DCLK1 expression was analyzed in the developing postnatal brain by Western blotting of WT mouse cortical lysates during stages of diminished spine remodeling in postnatal mice (P22-P34) and young adults (P50), as well as in older adults (P105) (Fig. 3A). Western

blotting for DCLK1 (equal amount of protein lysates) was carried out using an antibody to the carboxyl terminus of full length DCLK1 (82 kDa), which is shared by DCLK1-S (42 kDa). The full length DCLK1 isoform was prominently expressed at all time points in the mouse cortex, whereas DCLK1-S had a very minor presence and was also uniformly expressed. Densitometric quantification of DCLK1 82 kDa relative to actin in the blot shown in Fig. 3A indicated approximately similar levels of expression across postnatal development. DCLK1/actin ratios at each time point in 3 experiments were normalized by expressing them relative to values at P22 (1.0). The mean of these DCLK1 82 kDa/actin ratios ± SEM were not significantly different across the time course (1 factor ANOVA, $p=0.13$), as indicated below (Fig. 3A). The amount of DCLK1-S was too low to be reliably quantified.

The L1-CAM NrCAM has a known role in regulating dendritic spine density (Demyanenko *et al.*, 2014;Mohan *et al.*, 2019a). To examine a potential association of DCLK1 with NrCAM in the developing mouse cortex, NrCAM was immunoprecipitated from equal amounts of cortical lysates followed by immunoblotting for DCLK1, and reprobing for NrCAM (130 kDa). NrCAM and DCLK1 82 kDa co-immunoprecipitated from cortical lysates at each developmental stage (Fig. 3B). Nonimmune mouse IgG (NIg) did not immunoprecipitate DCLK1 or NrCAM as shown at P34 (Fig. 3B). DCLK1-S was not observed because it was obscured by the large IgG heavy chain band in the immunoprecipitates. Relative levels of co-immunoprecipitated DCLK1 and NrCAM in the experiment shown were generally consistent from P22 to P50, with an apparent increase in older adults (P105), as indicated by the densitometric ratios of DCLK1/NrCAM (Fig. 3B). DCLK1/NrCAM ratios at each time point in 3 experiments were normalized by expressing them relative to values at P22 (1.0). Mean DCLK1/NrCAM ratios ± SEM were not significantly different across the time course (1 factor ANOVA, $p=0.35$), as indicated below (Fig. 3B).

The association of DCLK1 with NrCAM was also examined by co-immunoprecipitation from lysates of synaptoneurosomes, a fraction from mouse forebrain (P28) that is enriched in pre- and postsynaptic terminals (Villasana *et al.*, 2006). DCLK1 (82 kDa) co-immunoprecipitated with NrCAM from synaptoneurosome lysates (Fig. 3C). A nonspecific band of higher molecular weight was evident in immunoprecipitates using either NrCAM antibodies or the nonimmune IgG control. Input blots showed DCLK1 (82 kDa) but not detectable levels of DCLK1-S in the synaptoneurosome fraction.The synaptoneurosome fractionation resulted in enrichment of the synapse-associated proteins SAP102 and PSD95 in the synaptoneurosome fraction (Syn) compared to the initial supernatant (S1) of the filtered homogenate of mouse brain (P28) (Fig. 3C right panel) as previously reported (Demyanenko *et al.*, 2014).

The conserved FIGQY motif in the cytoplasmic domain of all L1-CAMs reversibly binds Ankyrins (Bennett and Healy, 2009). Mutation of FIGQY to FIGQH in L1 is a human variant associated with the L1 syndrome of intellectual disability (Weller and Gartner, 2001). To test the binding of DCLK1 to NrCAM at this sequence, a tyrosine-1231 to histidine point mutation (Y1231H) was generated in NrCAM cDNA by site directed mutagenesis. HEK293T cells were transfected with expression plasmids for DCLK1 together with

WT NrCAM or NrCAM FIGQY^{1231}H. Cell lysates were assayed for association of NrCAM and DCLK1 by co-immunoprecipitation. Relative levels of DCLK1 and NrCAM in co-immunoprecipitates were quantified by densitometry. Results showed that DCLK1 co-immunoprecipitated efficiently with WT NrCAM but not with NrCAM FIGQY^{1231}H, (Fig. 3D). This finding indicated that DCLK1 interacts directly or indirectly with the NrCAM FIGQY motif.

The cytoskeletal adapter Ankyrin is established to bind all L1-CAMs at the motif FIGQY in the L1-CAM cytoplasmic domain (Bennett and Healy, 2009), and therefore might indirectly mediate NrCAM binding to DCLK1. To determine if DCLK1 associates with NrCAM indirectly through a potential interaction between DCLK1 and Ankyrin B, HEK293T cells were transfected with plasmids expressing DCLK1 and the ubiquitously expressed 220 kDa isoform of Ankyrin B (AnkB-220), then assayed for co-immunoprecipitation. Results revealed no association of DCLK1 with Ankyrin B (Fig.3E), supporting the interpretation that DCLK1 binds to the NrCAM FIGQY motif rather than indirectly through Ankyrin B.

Discussion

To investigate a role for DCLK1 in the regulation of dendritic spine development in cortical pyramidal neurons, we generated a novel conditional mutant mouse (Nex1Cre-ERT2: DCLK1$^{flox/flox}$: RCE) to delete microtubule-binding isoforms of DCLK1, including both full length and DCX-like isoforms, by Cre-mediated recombination of exon 3 under control of the tamoxifen-inducible Nex1 promoter in postmitotic, postmigratory pyramidal neurons. Homozygous or heterozygous inactivation of DCLK1 (P10-P13) decreased spine density on apical dendrites of layer 2/3 pyramidal neurons in the prefrontal cortex. Moreover, loss of DCLK1 preferentially decreased the fraction of mature (mushroom) spines and increased that of immature spines. DCLK1 and NrCAM were each expressed across postnatal and adult stages of mouse cortical development. DCLK1 was found to bind NrCAM at a conserved sequence FIGQY in its cytoplasmic domain, which is known to recruit the spectrin-actin adaptor Ankyrin. These results support a role for DCLK1 in facilitating spine growth and maturation during postnatal development of the prefrontal cortex.

The phenotype of DCLK1 F/F mice shares similarities and differences with other DCLK1 mouse models. Induction of recombination in Nex1Cre-ERT2: DCLK1 F/F mice at P10-P13 resulted in decreased spine density on apical dendrites of cortical pyramidal neurons but no alteration in cortical lamination, dendritic branching, or major axon tracts. Similarly, a global DCLK1 knockout mouse derived via homologous recombination in embryonic stem cells exhibited normal survival, gross brain architecture, and migration of neuronal progenitors (Deuel *et al.*, 2006). Excision of DCLK1 exon 3 in the EIIa-Cre: DCLK1 conditional mutant causes germline recombination and removes isoforms with microtubule-binding domains leaving the kinase-only isoform intact (Koizumi *et al.*, 2006). This mutant showed defects in formation of the corpus callosum and anterior commissure, most likely differing from our results due to the much earlier time of recombination.

In a different approach (Shin *et al.*, 2013) DCLK1 expression was downregulated by *in utero* shRNA expression under control of the human U6 promoter in neuronal progenitors, which

commenced at embryonic day E15.5, resulting in suppression of dendritic growth in the somatosensory cortex. An increase in spine density and width were reported but was notably small. In contrast postnatal deletion of DCLK1 in the Nex1Cre-ERT2 mouse line resulted in a significant decrease in spine density, which preferentially targeted mature spines, and did not decrease dendritic arborization. These differences are likely due the different stages of DCLK1 downregulation or deletion.

An interesting possibility is that DCLK1 in immature neural progenitors preferentially promotes dendritic growth, building the dendritic tree through microtubule transport of proteins for dendrite extension and arborization. Later, in differentiating pyramidal neurons, DCLK1 promotes spine growth and maturation using microtubules to transport proteins into developing spines via direct deposit or membrane diffusion (Dent, 2017). This scenario is in accord with the ability of DCLK1 to promote dendritic branching in neuronal cultures at early (DIV4) but not later (DIV9) time points (Shin *et al.*, 2013). It should be noted that any shRNA driven by the U6 promoter can cause toxicity of neurons in mice (Martin *et al.*, 2011), potentially affecting dendrite growth. Differences in phenotype between the mutants might also be due to diverse DCLK1 action in the distinct neocortical areas (somatosensory vs. prefrontal cortex) examined in these studies.

In the present study we show that DCLK1 binds to NrCAM at postnatal stages of development in the mouse neocortex. In transfected HEK393T cells this binding was dependent on the FIGQY motif within the NrCAM cytoplasmic domain. The lissencephaly protein DCX, which shares sequence homology with DCLK1 in the microtubule binding domains, was reported to bind the L1-CAM Neurofascin at the conserved FIGQY motif, but not NrCAM or L1, indicating specificity of association between L1-CAMs and DCX family members (Kizhatil *et al.*, 2002). The FIGQY motif is the location at which Ankyrin reversibly engages L1-CAMs (Bennett and Healy, 2009). Tyrosine phosphorylation of the FIGQY motif in Neurofascin decreases the affinity for Ankyrin allowing recruitment of DCX (Kizhatil *et al.*, 2002). DCLK1 did not co-immunoprecipitate with Ankyrin B from transfected HEK293 cells. More experiments are needed to determine if DCLK1 associates directly with NrCAM at this sequence.

DCLK1 might serve to promote or maintain spine growth and maturation during spine morphogenesis through its ability to transport dense core vesicles along microtubules (Lipka *et al.*, 2016). For example, DCLK1 may bind and transport NrCAM to the spine plasma membrane, positioning it for intercellular adhesion or spine pruning in response to activity-dependent expression of Sema3F (Mohan *et al.*, 2019a). With respect to additional modes of DCLK1 regulation, recent research has shown that DCLK1 auto-phosphorylates on its carboxyl terminal tail, which inhibits microtubule binding (Agulto *et al.*, 2021). Future studies with the Nex1Cre-ERT2: DCLK1$^{flox/flox:}$ RCE mice will be aimed at determining if loss of DCLK1 from pyramidal neurons impairs excitatory transmission or behavior due to reduction of spine density on apical dendrites of cortical pyramidal neurons in the prefrontal cortex. In addition, recent studies demonstrated that DCLK1 knockdown by shRNA in a mouse model of Parkinson's disease-like synucleopathy mitigates dopaminergic neurotoxicity and downregulates α-Synuclein levels post transcriptionally (Vazquez-Velez *et al.*, 2020). Since DCLK1 is a druggable target, Nex1Cre-ERT2: DCLK1$^{flox/flox}$: RCE mice

could be useful for investigating deleterious consequences of adult knockout of DCLK1 in pyramidal neurons.

Acknowledgements

This work was supported by the US National Institutes of Mental Health grant R01 MH113280 (PFM), UNC School of Medicine Biomedical Research Core Project award (PFM), and T32 NRSA (5T32HD040127–18) (KEM). Assistance for this project was provided by a UNC Intellectual and Developmental Disabilities Research Grant (NICHD P50HD1035731). We acknowledge Dr. Pablo Ariel, Director of the Microscopy Services Laboratory in the UNC Department of Pathology and Laboratory Medicine, who provided expert advice on imaging supported by P30 CA016086 Cancer Center Core Grant. We thank Dr. Gordon Fishell for providing the RCE mouse strain, and Alex Kampov-Polevoi and Harwinder Sidhu for technical assistance.

Abbreviations:

DCLK1	Doublecortin-like kinase-1
DCX	Doublecortin
NrCAM	Neuron-glia related cell adhesion molecule
Sema3	Semaphorin 3

References

Agarwal A, Dibaj P, Kassmann CM, Goebbels S, Nave KA, Schwab MH (2012). In vivo imaging and noninvasive ablation of pyramidal neurons in adult NEX-CreERT2 mice. Cereb Cortex 22:1473–1486. [PubMed: 21880656]

Agulto RL, Rogers MM, Tan TC, Ramkumar A, Downing AM, Bodin H, Castro J, Nowakowski DW, Ori-McKenney KM (2021). Autoregulatory control of microtubule binding in doublecortin-like kinase 1. Elife 10.

Bennett V, Healy J (2009). Membrane domains based on ankyrin and spectrin associated with cell-cell interactions. Cold Spring Harb Perspect Biol 1:1–19.

Berry KP, Nedivi E (2017). Spine Dynamics: Are They All the Same? Neuron 96:43–55. [PubMed: 28957675]

Bhatt DH, Zhang S, Gan WB (2009). Dendritic spine dynamics. Annu Rev Physiol 71:261–282. [PubMed: 19575680]

Bourne J, Harris KM (2007). Do thin spines learn to be mushroom spines that remember? Curr Opin Neurobiol 17:381–386. [PubMed: 17498943]

Culotta L, Penzes P (2020). Exploring the mechanisms underlying excitation/inhibition imbalance in human iPSC-derived models of ASD. Mol Autism 11:32. [PubMed: 32393347]

Demyanenko GP, Mohan V, Zhang X, Brennaman LH, Dharbal KE, Tran TS, Manis PB, Maness PF (2014). Neural Cell Adhesion Molecule NrCAM Regulates Semaphorin 3F-Induced Dendritic Spine Remodeling. J Neurosci 34:11274–11287. [PubMed: 25143608]

Demyanenko GP, Tsai AY, Maness PF (1999). Abnormalities in neuronal process extension, hippocampal development, and the ventricular system of L1 knockout mice. J Neurosci 19:4907–4920. [PubMed: 10366625]

Dent EW (2017). Of microtubules and memory: implications for microtubule dynamics in dendrites and spines. Mol Biol Cell 28:1–8. [PubMed: 28035040]

des Portes V, Pinard JM, Billuart P, Vinet MC, Koulakoff A, Carrie A, Gelot A, Dupuis E, Motte J, Berwald-Netter Y, Catala M, Kahn A, Beldjord C, Chelly J (1998). A novel CNS gene required for neuronal migration and involved in X-linked subcortical laminar heterotopia and lissencephaly syndrome. Cell 92:51–61. [PubMed: 9489699]

Deuel TA, Liu JS, Corbo JC, Yoo SY, Rorke-Adams LB, Walsh CA (2006). Genetic interactions between doublecortin and doublecortin-like kinase in neuronal migration and axon outgrowth. Neuron 49:41–53. [PubMed: 16387638]

Duncan BW, Mohan V, Wade SD, Truong Y, Kampov-Polevoi A, Temple BR, Maness PF (2021a). Semaphorin3F Drives Dendritic Spine Pruning Through Rho-GTPase Signaling. Mol Neurobiol 58:3817–3834. [PubMed: 33856648]

Duncan BW, Murphy KE, Maness PF (2021b). Molecular Mechanisms of L1 and NCAM Adhesion Molecules in Synaptic Pruning, Plasticity, and Stabilization. Front Cell Dev Biol 9:1–13.

Fame RM, MacDonald JL, Dunwoodie SL, Takahashi E, Macklis JD (2016). Cited2 Regulates Neocortical Layer II/III Generation and Somatosensory Callosal Projection Neuron Development and Connectivity. J Neurosci 36:6403–6419. [PubMed: 27307230]

Friocourt G, Liu JS, Antypa M, Rakic S, Walsh CA, Parnavelas JG (2007). Both doublecortin and doublecortin-like kinase play a role in cortical interneuron migration. J Neurosci 27:3875–3883. [PubMed: 17409252]

Goebbels S, Bormuth I, Bode U, Hermanson O, Schwab MH, Nave KA (2006). Genetic targeting of principal neurons in neocortex and hippocampus of NEX-Cre mice. Genesis 44:611–621. [PubMed: 17146780]

Golonzhka O, Nord A, Tang PLF, Lindtner S, Ypsilanti AR, Ferretti E, Visel A, Selleri L, Rubenstein JLR (2015). Pbx Regulates Patterning of the Cerebral Cortex in Progenitors and Postmitotic Neurons. Neuron 88:1192–1207. [PubMed: 26671461]

Havik B, Degenhardt FA, Johansson S, Fernandes CP, Hinney A, Scherag A, Lybaek H, Djurovic S, Christoforou A, Ersland KM, Giddaluru S, O'Donovan MC, Owen MJ, Craddock N, Muhleisen TW, Mattheisen M, Schimmelmann BG, Renner T, Warnke A, Herpertz-Dahlmann B, Sinzig J, Albayrak O, Rietschel M, Nothen MM, Bramham CR, et al. (2012). DCLK1 variants are associated across schizophrenia and attention deficit/hyperactivity disorder. PLoS One 7:e35424. [PubMed: 22539971]

Holtmaat A, Svoboda K (2009). Experience-dependent structural synaptic plasticity in the mammalian brain. Nat Rev Neurosci 10:647–658. [PubMed: 19693029]

Holtmaat AJ, Trachtenberg JT, Wilbrecht L, Shepherd GM, Zhang X, Knott GW, Svoboda K (2005). Transient and persistent dendritic spines in the neocortex in vivo. Neuron 45:279–291. [PubMed: 15664179]

Kizhatil K, Wu YX, Sen A, Bennett V (2002). A new activity of doublecortin in recognition of the phospho-FIGQY tyrosine in the cytoplasmic domain of neurofascin. J Neurosci 22:7948–7958. [PubMed: 12223548]

Koizumi H, Fujioka H, Togashi K, Thompson J, Yates JR 3rd, Gleeson JG, Emoto K (2017). DCLK1 phosphorylates the microtubule-associated protein MAP7D1 to promote axon elongation in cortical neurons. Dev Neurobiol 77:493–510. [PubMed: 27503845]

Koizumi H, Tanaka T, Gleeson JG (2006). Doublecortin-like kinase functions with doublecortin to mediate fiber tract decussation and neuronal migration. Neuron 49:55–66. [PubMed: 16387639]

Kroon T, van Hugte E, van Linge L, Mansvelder HD, Meredith RM (2019). Early postnatal development of pyramidal neurons across layers of the mouse medial prefrontal cortex. Sci Rep 9:5037. [PubMed: 30911152]

Laviola G, Macri S, Morley-Fletcher S, Adriani W (2003). Risk-taking behavior in adolescent mice: psychobiological determinants and early epigenetic influence. Neurosci Biobehav Rev 27:19–31. [PubMed: 12732220]

Lipka J, Kapitein LC, Jaworski J, Hoogenraad CC (2016). Microtubule-binding protein doublecortin-like kinase 1 (DCLK1) guides kinesin-3-mediated cargo transport to dendrites. EMBO J 35:302–318. [PubMed: 26758546]

Martin JN, Wolken N, Brown T, Dauer WT, Ehrlich ME, Gonzalez-Alegre P (2011). Lethal toxicity caused by expression of shRNA in the mouse striatum: implications for therapeutic design. Gene Ther 18:666–673. [PubMed: 21368900]

McVicker DP, Awe AM, Richters KE, Wilson RL, Cowdrey DA, Hu X, Chapman ER, Dent EW (2016). Transport of a kinesin-cargo pair along microtubules into dendritic spines undergoing synaptic plasticity. Nat Commun 7:12741. [PubMed: 27658622]

Miller DS, Wright KM (2021). Neuronal Dystroglycan regulates postnatal development of CCK/cannabinoid receptor-1 interneurons. Neural Dev 16:4. [PubMed: 34362433]

Mohan V, Sullivan CS, Guo J, Wade SD, Majumder S, Agarwal A, Anton ES, Temple BS, Maness PF (2019a). Temporal Regulation of Dendritic Spines Through NrCAM-Semaphorin3F Receptor Signaling in Developing Cortical Pyramidal Neurons. Cereb Cortex 29:963–977. [PubMed: 29415226]

Mohan V, Wade SD, Sullivan CS, Kasten MR, Sweetman C, Stewart R, Truong Y, Schachner M, Manis PB, Maness PF (2019b). Close Homolog of L1 Regulates Dendritic Spine Density in the Mouse Cerebral Cortex Through Semaphorin 3B. J Neurosci 39:6233–6250. [PubMed: 31182634]

Nedivi E, Hevroni D, Naot D, Israeli D, Citri Y (1993). Numerous candidate plasticity-related genes revealed by differential cDNA cloning. Nature 363:718–722. [PubMed: 8515813]

Patel O, Dai W, Mentzel M, Griffin MD, Serindoux J, Gay Y, Fischer S, Sterle S, Kropp A, Burns CJ, Ernst M, Buchert M, Lucet IS (2016). Biochemical and Structural Insights into Doublecortin-like Kinase Domain 1. Structure 24:1550–1561. [PubMed: 27545623]

Peters A, Harriman KM (1990). Different kinds of axon terminals forming symmetric synapses with the cell bodies and initial axon segments of layer II/III pyramidal cells. I. Morphometric analysis. J Neurocytol 19:154–174. [PubMed: 2358827]

Peters A, Kaiserman-Abramof IR (1970). The small pyramidal neuron of the rat cerebral cortex. The perikaryon, dendrites and spines. Am J Anat 127:321–355. [PubMed: 4985058]

Shin E, Kashiwagi Y, Kuriu T, Iwasaki H, Tanaka T, Koizumi H, Gleeson JG, Okabe S (2013). Doublecortin-like kinase enhances dendritic remodelling and negatively regulates synapse maturation. Nat Commun 4:1440. [PubMed: 23385585]

Sousa VH, Miyoshi G, Hjerling-Leffler J, Karayannis T, Fishell G (2009). Characterization of Nkx6–2-derived neocortical interneuron lineages. Cereb Cortex 19 Suppl 1:i1–10. [PubMed: 19363146]

Trachtenberg JT, Chen BE, Knott GW, Feng G, Sanes JR, Welker E, Svoboda K (2002). Long-term in vivo imaging of experience-dependent synaptic plasticity in adult cortex. Nature 420:788–794. [PubMed: 12490942]

Tran TS, Rubio ME, Clem RL, Johnson D, Case L, Tessier-Lavigne M, Huganir RL, Ginty DD, Kolodkin AL (2009). Secreted semaphorins control spine distribution and morphogenesis in the postnatal CNS. Nature 462:1065–1069. [PubMed: 20010807]

Vazquez-Velez GE, Gonzales KA, Revelli JP, Adamski CJ, Alavi Naini F, Bajic A, Craigen E, Richman R, Heman-Ackah SM, Wood MJA, Rousseaux MWC, Zoghbi HY (2020). Doublecortin-like Kinase 1 Regulates alpha-Synuclein Levels and Toxicity. J Neurosci 40:459–477. [PubMed: 31748376]

Villasana LE, Klann E, Tejada-Simon MV (2006). Rapid isolation of synaptoneurosomes and postsynaptic densities from adult mouse hippocampus. J Neurosci Methods 158:30–36. [PubMed: 16797717]

Weller S, Gartner J (2001). Genetic and clinical aspects of X-linked hydrocephalus (L1 disease): Mutations in the L1CAM gene. Hum Mutat 18:1–12. [PubMed: 11438988]

Yap CC, Vakulenko M, Kruczek K, Motamedi B, Digilio L, Liu JS, Winckler B (2012). Doublecortin (DCX) mediates endocytosis of neurofascin independently of microtubule binding. J Neurosci 32:7439–7453. [PubMed: 22649224]

Yap CC, Winckler B (2015). Adapting for endocytosis: roles for endocytic sorting adaptors in directing neural development. Front Cell Neurosci 9:119. [PubMed: 25904845]

Yizhar O (2012). Optogenetic insights into social behavior function. Biol Psychiatry 71:1075–1080. [PubMed: 22341368]

Highlights

- Doublecortin-like kinase 1 (DCLK1) promotes spine development in mouse cortex. 79 characters with spaces
- An inducible mouse line was generated to delete DCLK1 isoforms from cortical pyramidal neurons. 97 characters with spaces.
- DCLK1 binds the cell adhesion molecule NrCAM at its Ankyrin interaction motif. 79 characters with spaces.

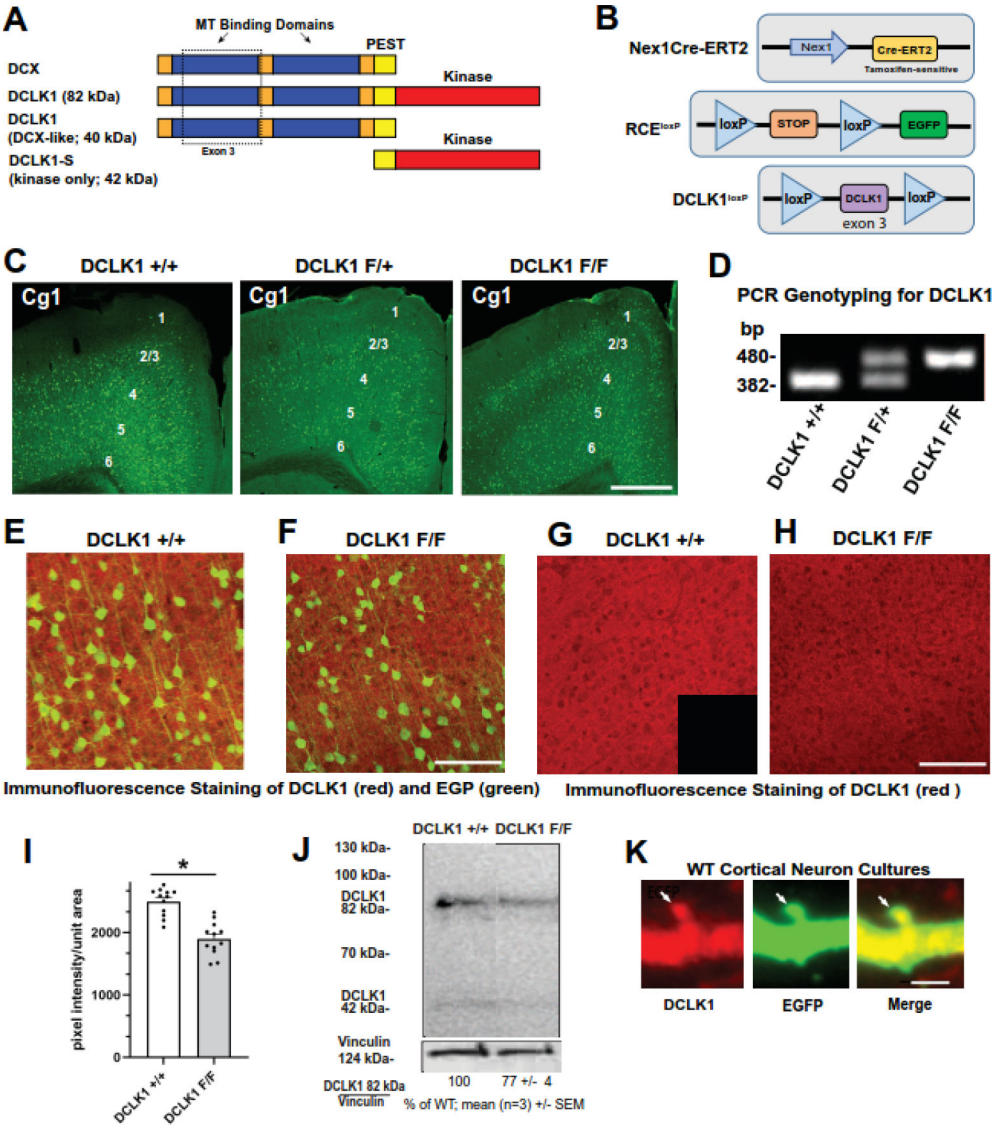

Figure 1: Conditional deletion of DCLK1 in postnatal pyramidal neurons of Nex1Cre-ERT2: DCLK1 F/F: RCE mice.

(A) DCX and DCLK1 isoforms and domain structure. MT, microtubule; PEST sequence; kinase, serine/threonine kinase domain; dotted box, exon3 encoded sequences.

(B) Cre-Lox diagram for recombination in Nex1Cre-ERT2: DCLK1 F/F: RCE mice. Nex1Cre-ERT2 mice express an estrogen/tamoxifen-sensitive Cre recombinase from the endogenous Nex1 promoter in postmitotic pyramidal neurons. These mice were intercrossed with RCE:loxP mice in which EGFP is inducibly expressed in the same neurons due to Cre-ERT2-mediated recombination of a STOP sequence flanked by loxP sites. Mice were also intercrossed with DCLK1 floxed mice in which exon 3 of DCLK1 is flanked by loxP sites, which is recombined out in the same neurons upon tamoxifen induction.

(C) Recombination in DCLK1 +/+ (WT), DCLK1 F/+ and DCLK1 F/F in the cingulate cortex (Cg1; P24) of prefrontal cortex indicated by EGFP expression in the indicated cortical layers after tamoxifen induction at P10–13. Scale bar = 100 μm.

(D) PCR genotyping was used to identify exon 3 excision in DCLK1 genomic DNA extracted from DCLK1 +/+, F/+ and F/F mice, as indicated by the size in base pairs (bp) of diagnostic bands on agarose gels.

(E-F) Immunofluorescence staining of DCLK1 protein (red) in EGFP-expressing pyramidal neurons (green) in Cg1 layer 2/3 of DCLK1 +/+ and DCLK1 F/F mice after tamoxifen induction, shown in representative merged confocal images. Scale bar in F = 100 μm. DCLK1 recombination results in decreased DCLK1 immunostaining.

(G-H) Single channel DCLK1 immunofluorescence staining (red) in confocal images of DCLK1 +/+ and DCLK1 F/F Cg1 layer 2/3 after tamoxifen induction as in E,F. A secondary antibody control without primary antibodies is shown as an inset in G at the same confocal settings. DCLK1 staining is decreased in DCLK1 F/F brain compared to DCLK1 +/+ and both genotypes show DCLK1 immunofluorescence that is greater than the negative control. Scale bar= 100 μm.

(I) Quantification of pixel intensity of single channel DCLK1 immunofluorescence staining in DCLK1 +/+ and DCLK1 F/F Cg1 after tamoxifen induction. Quantification of pixel intensity shows a significantly (*) decreased mean pixel intensity per unit area in DCLK1 F/F compared to DCLK1 +/+ Cg1 layer 2/3 (2-tailed t-test, $p < 0.0001$). Each point corresponds to pixel intensity per unit area on 12 images per genotype (n=3 mice per genotype).

(J) Comparison of DCLK1 protein in a representative Western blot of cortical lysates from DCLK1 +/+ and DCLK1 F/F mice (P25) probed with DCLK1 antibodies, followed by reprobing with vinculin antibodies as a loading control (lower panel). Below: ratio of DCLK1 (82 kDa) /vinculin in scanned blots of cortical lysates (n= 3 /genotype) expressed as mean percent of DCLK1 +/+ (± SEM). The mean difference in the ratio of DCLK1 82 kDa/vinculin was significant between genotypes (t-test, 2-tailed, $p < 0.0001$).

(K) Confocal image of an apical dendrite segment of an EGFP-expressing neuron in primarly cortical cultures. WT cortical neuronal cultures at DIV14 were transfected with pCAG-IRES-EGFP, fixed, immunostained for DCLK1 (red) and EGFP (green), and imaged confocally. Images from individual and merged channels are shown. DCLK1 immunoreactivity was present on dendritic shafts and spines as shown in this representative image. Arrows indicate a mushroom-shaped spine on the apical dendrite. Scale bar = 1 μm

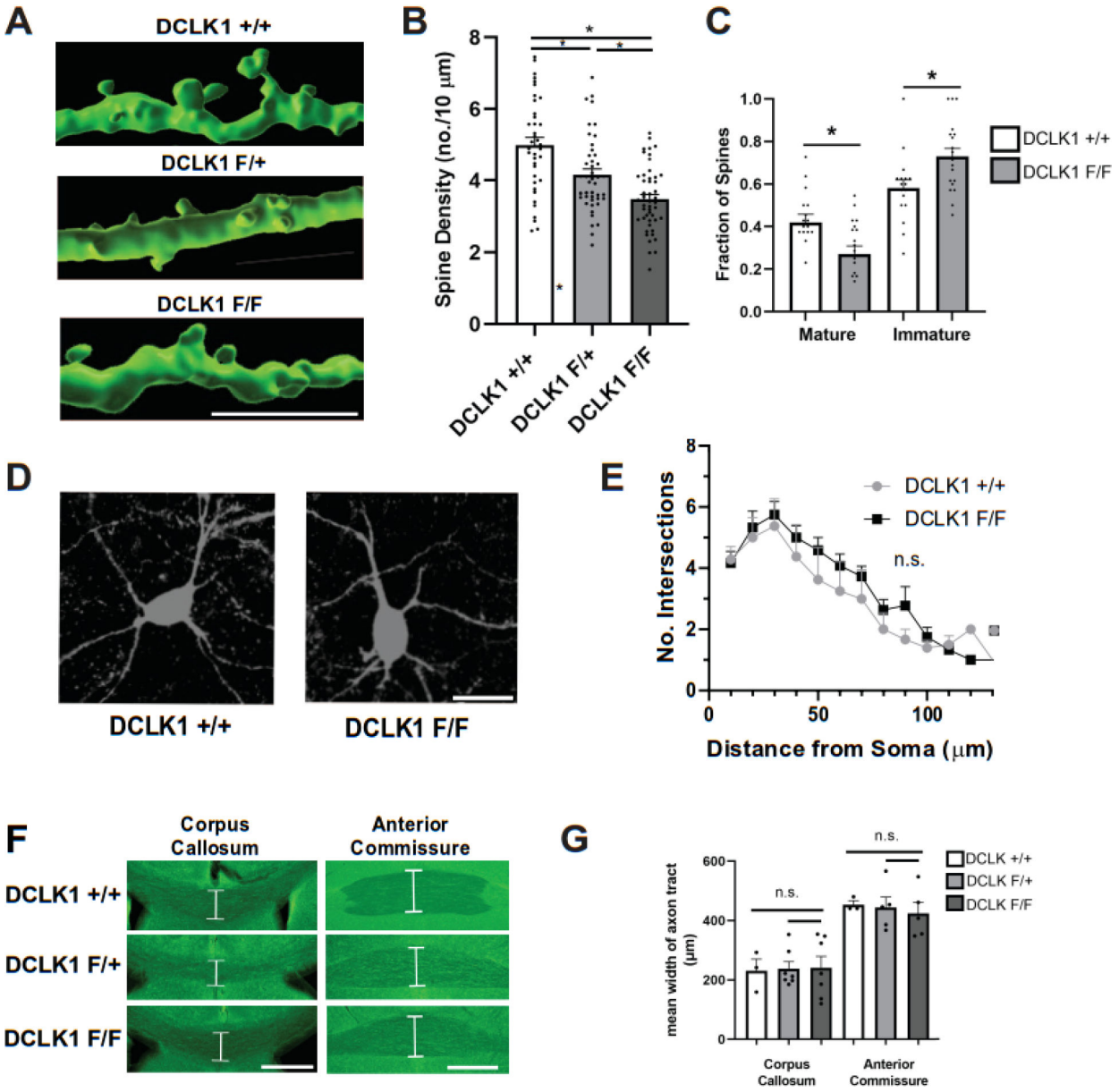

Figure 2: Decreased spine density and mature synapses on apical dendrites in DCLK1 mutant pyramidal neurons in PFC layer 2/3.

(A) 3D reconstructions of EGFP-labeled apical dendrites and spines on representative pyramidal neurons in layer 2/3 of prefrontal cortex of DCLK1 +/+, F/+, and F/F mice induced at P10-P13 and analyzed at P19–34. Scale bar = 10 µm.

(B) Quantification of mean spine density ± SEM on GFP-labeled apical dendrites of layer 2/3 pyramidal neurons in PFC layer 2/3 of DCLK1 +/+, F/+, and F/F mice. Each point represents the mean spine density on apical dendrites of single GFP-expressing pyramidal neurons in 4 DCLK1 +/+ mice, 4 DCLK1 F/+ mice, and 6 DCLK1 F/F mice (P19–34) (* significant differences, $p < 0.001$, 1 factor ANOVA with Tukey's posthoc comparisons). DCLK1 +/+ vs. DCLK1 F/+ $p=0.0016$; DCLK1 +/+ vs. DCLK1 F/F $p < 0.0001$, DCLK1

F/+ vs. DCLK1 F/F p=0.011). Approximately 39–49 neurons/genotype were analyzed per genotype.

(C) Quantification of spine morphologies on apical dendrites of layer 2/3 pyramidal neurons in the prefrontal cortex showed a significant decrease in the fraction of mature (mushroom) spines of DCLK1 F/F compared to DCLK1 +/+ mice (*p=0.01) and a significant increase in the fraction of immature (thin and stubby) spines (*p=0.01) (3 DCLK1 +/+ and 4 DCLK1 F/F mice were induced at P10-P13 and analyzed at P19–34). Each point corresponds to a single neuron. Approximately 146 spines per genotype and 17–19 neurons/mouse were analyzed.

(D) Representative images of EGFP-labeled pyramidal neurons and their proximal arbors in layer 2/3 of DCLK1 +/+ and DCLK1 F/F prefrontal cortex, layer 2/3 are shown converted to black and white for better visualization of the processes. Scale bar = 50 μm.

(E) Sholl analysis for branching of processes in EGFP-labeled layer 2/3 pyramidal neurons in the prefrontal cortex showed a non-significant (n.s.) difference between DCLK1 +/+ and DCLK1 F/F mice (15 neurons/genotype, 3 mice/genotype, P19-P34), as indicated by paired t-test comparisons of the mean number of intersections at each distance from the soma ($p > 0.05$).

(F) The widths of the corpus callosum (CC) and anterior commissure (AC) (white brackets) were measured at the midline in serial coronal brain sections of DCLK1 +/+, F/+, and F/F mice (P19–34) expressing EGFP after tamoxifen induction at P10-P13. Scale bar = 300 μm.

(G) DCLK1 F/F mice showed no change in mean width of the corpus callosum or anterior commissure compared to DCLK1 +/+ or DCLK1 F/+ mice (1 factor ANOVA with Tukey's post hoc tests; $p > 0.05$). 3–5 mice were analyzed/genotype (indicated by points). Non-significant (n.s.) differences are indicated by bars. For corpus callosum group comparisons, p-values were greater than 0.99. For anterior commissure group comparisons DCLK+/+ vs. F/F p=0.57, +/+ vs. F/+ $p > 0.99$, F/+ vs. F/F p=0.69.

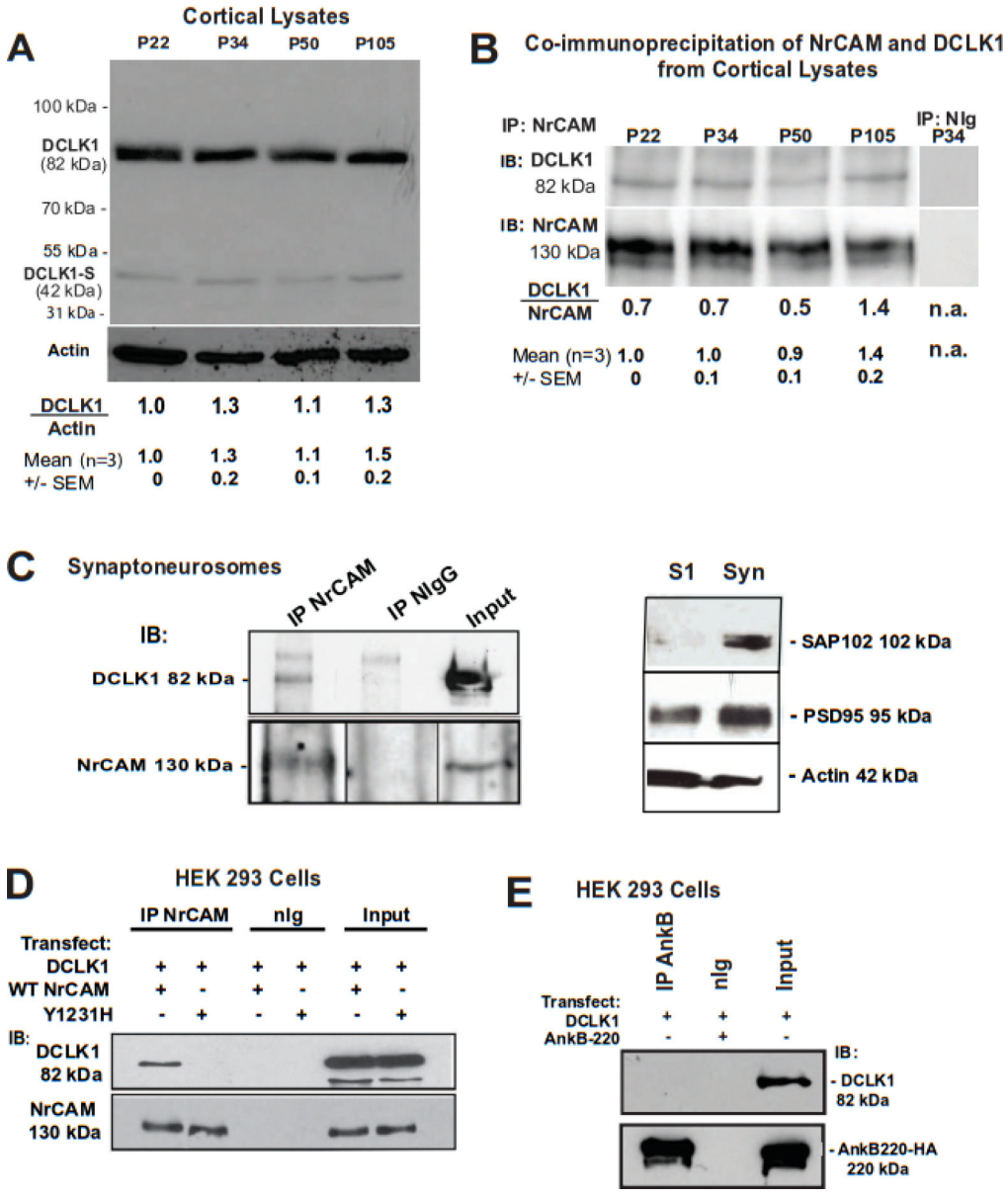

Figure 3: DCLK1 expression and binding to NrCAM at the FIGQY motif.

(A) Time course of DCLK1 expression in developing mouse cortex. Western blotting of equal amounts of protein in lysates of mouse cortex showed expression of DCLK1 (82 kDa) and DCLK1-S (42kDa) at postnatal stages P22, 34, 50 and older adulthood P105. The blot was reprobed for actin as a loading control. Densitometric scanning and quantitation of band intensities indicated comparable ratios of DCLK1 (82 kDa) to actin (below). DCLK1/actin ratios at each time point from 3 experiments were normalized relative to values at P22 (1.0). Mean ratios at each time point were not significantly different (1 factor ANOVA, p=0.13). (B) Co-immunoprecipitation of DCLK1 (82 kDa) with NrCAM from mouse cortex lysates at postnatal stages P22, P34, P50 and P105. NrCAM was immunoprecipitated (IP) from equal amounts of protein lysates, and immunoblotted (IB) for DCLK1. Blots were reprobed for NrCAM (130 kDa, lower panel). Nonimmune IgG (NIg) did not pull down detectable

amounts of DCLK1 or NrCAM, as shown for the P34 lysate. Densitometric scanning indicated comparable ratios of DCLK1 to NrCAM in the immunoprecipitates from P22-P50, with an apparent increase at P105. A ratio in the NIg control was not applicable (n.a.). DCLK1/NrCAM ratios at each time point in 3 experiments were normalized relative to values at P22 (1.0). Mean DCLK1/NrCAM ± SEM were not significantly different across the time course (1 factor ANOVA, p=0.35).

(C) Association of DCLK1 (82kDa) and NrCAM (130 kDa) from mouse brain synaptoneurosomes (P28) (equal amounts of protein) was shown by immunoprecipitation (IP) of NrCAM with NrCAM antibodies or NIgG (control), followed by immunoblotting (IB) with DCLK1 antibodies. Blots were reprobed for NrCAM (lower panel). Input lysate blots are also shown. No DCLK1-S was observed in synaptoneurosome lysates. In the panel at right, fractionation of P28 mouse brain produced a clarified supernatant (S1) of the filtered brain homogenate, followed by subsequent detergent lysis and higher speed centrifugation to yield the synaptoneurosome fraction (Syn). Western blotting of equal amounts of protein in S1 and Syn fractions validated the enrichment of postsynaptic density proteins SAP102 (102 kDa) and PSD95 (95 kDa) in the Syn fraction. Blots were reprobed for actin as a loading control.

(D) HEK293T cells were transfected with cDNAs encoding DCLK1 and WT NrCAM, or DCLK1 and mutant NrCAM $Y^{1231}H$. Cell lysates (equal protein) were immunoprecipitated with NrCAM antibodies (IP) or NIgG, and Western blots probed with DCLK1 antibodies. DCLK1 co-immunoprecipitated with WT NrCAM but not mutant NrCAM $Y^{1231}H$. Blots were reprobed for NrCAM (lower panel). Input lysate blots showed comparable levels of expression of DCLK1 and NrCAM in WT and mutant HEK293 cells.

(E) HEK293T cells were transfected with AnkB 220-HA and/or DCLK1 cDNAs, immunoprecipitated (IP) with Ankyrin B antibodies or NIgG, and immunoblotted (IB) for DCLK1. Blots were reprobed for AnkyrinB below. The input lysate is shown at the right. DCLK1 did not detectably co-immunoprecipitate with Ankyrin B-220 even at prolonged exposures of film by enhanced chemiluminescence.